E3S Web of Conferences **728**, 01001 (2026) https://doi.org/10.1051/e3sconf/202672801001
EEUPD 2026

Simulation Study of Refraction Seismic Wave Testing for Geophysical Exploration

Lanlan Qin [1], Chen-Yuan Chiu [1,*], Nan Zhang[1], Ziwei Luo [1], Changfa Cai [2]

[1] College of Civil Engineering, Jiaying University, Meizhou 514015, China
[2] Building Materials Guangzhou Engineering Survey Institute Co., Ltd., Guangzhou, 510403 China

Abstract. This study investigates the application of the refraction seismic method for geophysical exploration in engineering geology. By analyzing time-distance curves generated from seismic wave propagation, we determined the stratigraphic velocity layers and structural boundaries at a highway interchange improvement project site. Two survey lines (L-1 and L-2) were established, with seismic waves generated by hammer impacts. The delay time method was employed to calculate velocity profiles, revealing four distinct layers: overburden, coarse sand with gravel, weathered rock, and interbedded sandstone-mudstone. Results demonstrate the efficacy of refraction seismography in detecting shallow stratigraphy and identifying low-velocity zones, providing critical data for engineering design and construction.

1 Introduction

The refraction seismic method is a cornerstone of geophysical exploration, enabling subsurface characterization through the analysis of artificially generated seismic waves. This technique relies on the principle that seismic waves refract at interfaces between geological layers with contrasting velocities, governed by Snell's law [1]. Early applications of refraction seismics focused on mapping bedrock depths and detecting large-scale structural features [2]. Over time, advancements in data acquisition and inversion algorithms have enhanced its resolution, making it indispensable for engineering geology, particularly in infrastructure projects requiring precise stratigraphic delineation [3,4].

These methods include Horizontal to Vertical Spectral Ratio (HVSR) techniques, seismic refraction and Multi-channel Analysis of Surface Waves (MASW) measurements [5,6], and Resistivity Tomography (ERT) measurements. The shallow seismic refraction (SSR) technique is commonly used in similar studies [7] and is considered one of the main geophysical methods for studying subsurface lithologic structures. The propagation of elastic waves makes it possible to determine their velocities in soil sediments and rocks and also to calculate the corresponding elastic modulus. These methods are fast and reliable and have been used in the past for field characterization of seismic stations [8,9]. Geophysical methods are often preferred because they are much less costly than geotechnical methods that collect data from boreholes.

2 Methodology

The refraction seismic method is based on the explosion of explosives (or the impact of falling hammers) to generate artificial seismic waves, which are propagated in the underground strata. Due to the different velocities of the seismic waves in the strata, refraction occurs according to Snell's law and returns to the surface, where they are received by the receiver buried in the ground, and are then followed by the time-distance relationship (commonly referred to as time-distance curves), in order to find out the geological structure of the strata.

The basic model is used to explore the principle of calculating the stratigraphic structure from the time-distance curve (Fig. 1).

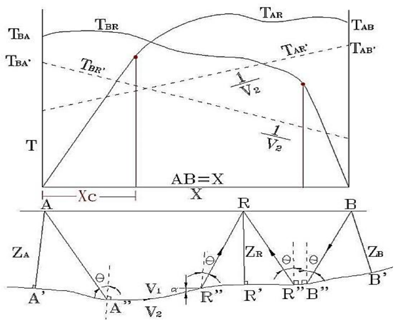

Fig. 1. Principle of refractive seismography

Setting A and B as the bomb points, R as the wave-receiving point, θ as the critical angle, and the vertical distances from the V_2 layer at each point of A, B, and R as Z_A, Z_B, and Z_R, and utilizing the delay time method to find out the stratigraphic velocity, depth, and the change of stratigraphic shapes. Assuming that the travel time from point A to point R is T_{AR}, the travel time from point B to point R is T_{BR}, and the travel time from point A to

* Corresponding author: maachiu@163.com

point B is T_{AB}, these three values can be expressed in the following formula:

$$T_{AR} = \frac{Z_A \cos\theta}{V_1} + \frac{Z_R \cos\theta}{V_1} + \frac{1}{V_2}\int_A^R \frac{dx}{\cos\alpha} \quad (1)$$

$$T_{BR} = \frac{Z_B \cos\theta}{V_1} + \frac{Z_R \cos\theta}{V_1} + \frac{1}{V_2}\int_B^R \frac{dx}{\cos\alpha} \quad (2)$$

$$T_{AB} = \frac{Z_A \cos\theta}{V_1} + \frac{Z_B \cos\theta}{V_1} + \frac{1}{V_2}\int_A^B \frac{dx}{\cos\alpha} \quad (3)$$

where α is the dip angle of stratigraphic change.

Assuming:

$$Y = T_{AR} + T_{BR} - T_{AB},$$

then

$$Y = 2\frac{Z_R \cos\theta}{V_1},\ Z_R = \frac{V_1 Y}{2\cos\theta} \quad (4)$$

Assume also:

$$T_{AR'} = T_{AR} - \frac{Y}{2}$$

$$T_{BR'} = T_{BR} - \frac{Y}{2}$$

then

$$T_{AR'} = \frac{Z_A \cos\theta}{V_1} + \frac{1}{V_2}\int_A^R \frac{dx}{\cos\alpha} \quad (5)$$

then

$$T_{BR'} = \frac{Z_B \cos\theta}{V_1} + \frac{1}{V_2}\int_B^R \frac{dx}{\cos\alpha} \quad (6)$$

Except for very drastic stratigraphic changes, usually Cos α ≒ 1, then the above equation is:

$$T_{AR'} = \frac{Z_A \cos\theta}{V_1} + \frac{X}{V_2} \quad (7)$$

$$T_{BR'} = \frac{Z_B \cos\theta}{V_1} + \frac{AB-X}{V_2} \quad (8)$$

Where X is the horizontal distance from point A to point R, AB is the horizontal distance from point A to point B. From the above equation, we can see that the slope of $T_{AR'}$ and $T_{BR'}$ is $\frac{1}{V_2}$, so we can find out the value of V_2 from the velocity time curve, and the depth of the second layer of each test point R is $Z_B = \frac{V_1(T_{AR}-T_{BR})}{\cos\theta}$, from which we can find out the second layer of the layer of the continuous profile.

The refraction seismic method is the most effective method for the exploration of fracture zones and faults in engineering geological investigations.

3 Case Survey Line Layout

The stratigraphic distribution at the study site can be divided into approximately four levels within the investigated depth:

(1) Cover soil layer and backfill layer:

The overburden layer is distributed in the higher-elevation area adjacent to the existing expressway on the northwest side of the construction site (i.e., the area where refraction seismic surveys were conducted), with terraced deposits and bedrock beneath it. Given the proximity to the expressway, it is inferred that localized backfilling occurred during the expressway's construction. Based on material analysis, the backfill likely originated from excavated material near the site, making it difficult to distinguish between backfill and overburden layers by material composition alone. Preliminary investigation data indicates this layer locally contains gravel and slag. Based on drilling and seismic survey results, this layer has a thickness ranging from 0 to 6.0 meters. Its primary composition consists of yellowish-brown to reddish-brown silty sand occasionally interbedded with gravel. Standard penetration test (SPT) N-values range from 7 to 13. Laboratory physical property tests indicate that, according to the Unified Soil Classification System, the fine-grained material in this layer predominantly falls under SM and ML categories. The natural moisture content is approximately 20%, the void ratio is about 0.50, and the unit weight is approximately 2.10 t/m³.

(2) Alluvial soil layer:

Alluvial soil layers are distributed across the gently sloping lowlands southeast of the expressway. Analysis indicates these layers were formed by recent alluvial deposits from stream transport. Supplementary survey data from boreholes near the expressway show an alluvial soil thickness of 5.2 meters, with a total alluvial layer thickness of 12.45 meters overlying soft rock strata.

Standard penetration test (SPT) N-values for this layer range from 3 to 30, with an average of approximately 17. The layer primarily consists of yellowish-brown to yellowish-gray or gray silty sand and clay. According to laboratory tests of general physical properties, most of this layer falls under the CL classification in the Unified Soil Classification System, with a small portion classified as SM. The natural moisture content ranges from approximately 20.5% to 34.4%, averaging about 26.2%. The void ratio ranges from 0.42 to 0.90, averaging approximately 0.70; unit weight ranges from 1.78 to 2.16 t/m³, averaging approximately 2.02 t/m³. The liquid limit and plasticity index ranged from 32 to 43 and 13 to 18, respectively. Direct shear strength tests conducted on disturbed soil samples obtained using a cable-type core sampler yielded shear strengths C = 0.9 to 1.7 tf/m² and ψ = 25.5° to 30.3°.

(3) Terrace Deposits

This layer is distributed in the higher-elevation area northwest of the construction site adjacent to the existing expressway (i.e., the area where refraction seismic surveys were conducted), with bedrock beneath it. It is determined that the terrace deposits on this elevated terrain represent early alluvial deposits. Over time, the gravel and cementing materials within these terrace deposits have undergone prolonged weathering and leaching, resulting in lateritic weathering and a coloration ranging from yellowish-brown to reddish-brown. The standard penetration test (SPT) N-values for this layer range from 3 to 30, with an average of approximately 17. The layer primarily consists of yellowish-brown silty loam containing medium to coarse sand interbedded with gravel, occasionally interspersed with thin clay layers. The SPT N-values for this layer vary significantly depending on the amount of gravel present, ranging from 8 to >50, with an average of approximately 24. Based on laboratory physical property test results, most fine materials in this layer belong to SM according to the Unified Soil Classification System. The natural moisture content ranges from approximately 13.8% to 21.5%, averaging about 17.9%. The void ratio ranges from 0.46 to 0.75, averaging approximately 0.55. Unit weight ranges from 1.75 to 2.06 t/m³, averaging approximately 1.98 t/m³. Direct shear strength tests conducted on disturbed soil samples with lower gravel content, obtained using a cable-type core sampler, yielded fine material shear strengths C = 6.0–7.3 tf/m² and ψ = 35.9°–39.9°.

(4) Rock formation

This investigation encountered soft rock layers beneath the alluvial deposits and terrace accumulations. According to the attached regional geological map, the study area is situated within the Erzhongxi Formation, characterized by sandstone dominated lithology with localized interbedding of blue-gray mudstone. Occasional small gravels are observed in layered arrangements. Based on drilling data from this investigation, the rock layers consist primarily of yellowish-brown to gray muddy siltstone and mudstone. Some sandstone and mudstone thin layers form closely interbedded thin interlayers. Additionally, a 0.75-meter-thick gravel interlayer was encountered in borehole BH-4. Based on drill core analysis, the bedding planes exhibit a dip angle of approximately 15° to 25°.

Due to the recent geological age of the Erzhongxi Formation, the rock is generally soft, poorly cemented, and exhibits minimal jointing. Field standard penetration test (SPT) N-values indicate values between 20 and 50 for sandstone layers, while mudstone layers exhibit N-values exceeding 50. Uniaxial compression tests reveal uniaxial compressive strengths ranging from 12.1 to 37.9 tf/m² for sandstone and 56.2 to 100.1 tf/m² for mudstone. Due to disturbance from drilling and sampling, which often affects the cementation of weak rock layers (especially loose sandstone), the actual rock strength is likely higher than the test values.

Based on rock direct shear test results, the peak cohesion (Cp) of weak sandy mudstone layers is 15–16 tf/m², with friction angle (∮ p) ranging from 33.5° to 39.5°. The residual cohesion (Cr) of the sandy mudstone layers is 1.0–4.0 tf/m², with a friction angle (∮ r) of 32.0–34.6°. Given the loose nature of the weak sandstone layers and the even greater weakness of the weathered rock layers, these can be treated as dense soil layers in engineering design.

In this study, two refraction seismic survey lines were set up at the site (the locations are shown in Fig. 2), i.e., L-1 (100m) and L-2 (100m), with a total length of 200 meters and a spacing of 5 meters between oscilloscope points. The seismic wave was generated by hammering the seismic source, and several hammering points were set up in each line. The purpose of setting up several hammering points in the lines is to accurately detect the shallow stratigraphy and prevent the interpretation of the deeper structure from errors due to the complexity of the shallow local structure. The purpose of setting up several hammering points in the survey line is to detect the shallow stratigraphic structure in detail and accurately, so that the interpretation of the deeper stratigraphic structure will not be inaccurate due to the complexity of the shallow local structure, and the seismic wave data from different hammering points can be verified with each other to find out the correct stratigraphic structure.

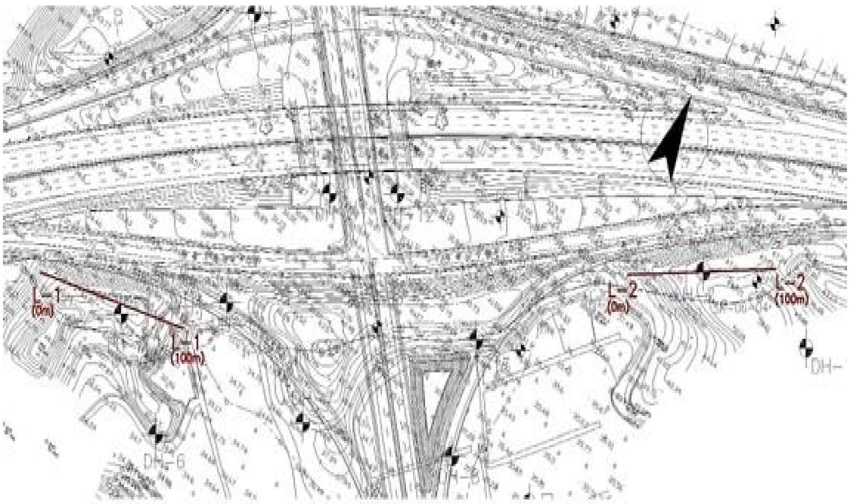

Fig. 2. Geophysical Survey Location Map

4 Results and Discussion

The seismic wave record of each seismic survey line is plotted as a time-distance curve by reading the initial wave travel time of each test point under different hammering points, and the velocity time-distance curve of the line is calculated by the delay time method. The velocity time-distance curve can be used to determine the boundary of different velocity layers and the boundary of the low-velocity zones, and at the same time, the thickness and velocity of the velocity layers are also calculated, and the possible response of the velocity layers are also estimated. The lithology is described as follows:

(1) The velocity layer profile of the L-1 survey line is shown in Fig. 3, and the shock wave propagation time curve is shown in Fig. 4, which can be divided into three velocity layers:

- The first layer of overburden: thickness between 3 and 6 meters, seismic wave velocity between 0.42 and 0.47 km/sec.
- The second layer of coarse sand with gravel: thickness between 4 and 9 meters, seismic wave velocity between 1.28 and 1.43 km/sec.
- The thickness of the third weathered rock layer ranges from 3 to 8 meters, and the seismic wave velocity is 1.88 km/sec.
- Interbedded sandstone and mudstone of the fourth layer: the velocity of the seismic wave is 2.05-2.35 km/sec, with lower velocities between 30 m and 45 m on the survey pile and between 65 m and 85 m on the survey pile.

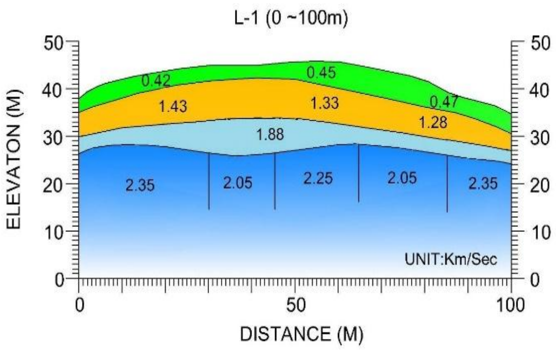

Fig. 3. Velocity layer profile of L-1 line seismic survey results

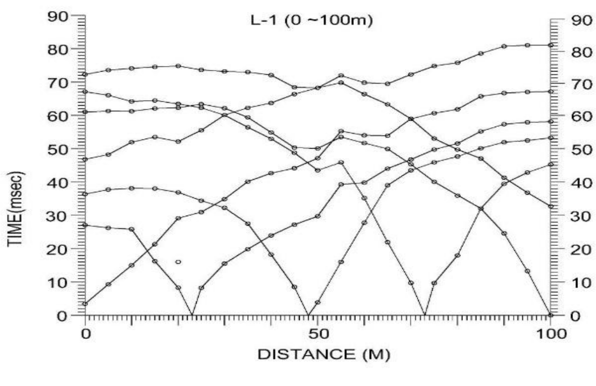

Fig. 4. L-1 Shock Wave Traveling Time Curves

(2) The velocity layer profile of the L-2 survey line is shown in Fig. 5, and the shock wave propagation time curve is shown in Fig.6, which can be divided into three velocity layers:

- First overburden layer: thickness between 3 and 4 meters, seismic velocity between 0.33 and 0.43 km/sec.
- The second layer is a layer of coarse sand with gravel: the thickness ranges from 5 to 7 meters, and the velocity of the seismic wave ranges from 1.53 to 1.73 km/sec.
- The third weathered rock layer: thickness between 4 and 13 meters, seismic wave velocity between 2.05 and 2.15 km/sec.
- The fourth layer of sandstone with mudstone: the seismic wave velocity ranges from 2.52 to 2.64 km/sec, and the rock layer is relatively uniform.

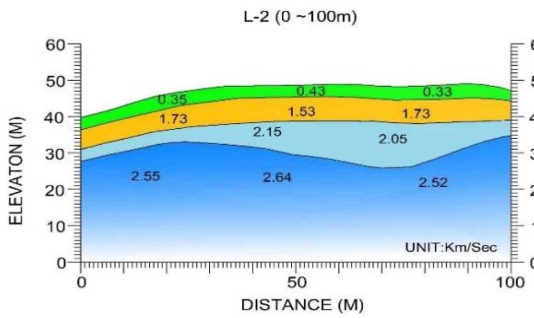

Fig. 5. Velocity layer profile of L-2 line seismic survey results

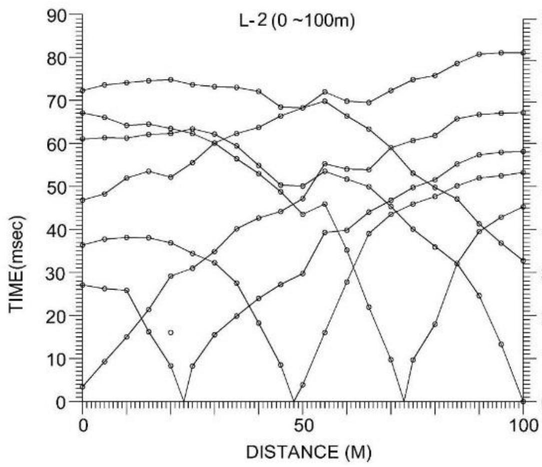

Fig. 6. L-2 Shock Wave Traveling Time Curves

5 Conclusions

The refraction seismic method successfully identified four velocity layers at the study site, with seismic wave velocities ranging from 0.33 km/s (overburden) to 2.64 km/s (sandstone-mudstone layer). Key findings include:

- Shallow layers (3–6 m thick) exhibited low velocities (0.33–0.47 km/s), consistent with unconsolidated overburden.
- Intermediate layers (coarse sand with gravel) showed moderate velocities (1.28–1.73 km/s), indicating compacted sedimentary deposits.
- Deeper weathered rock and sandstone-mudstone layers displayed higher velocities (1.88–2.64 km/s), correlating with lithological homogeneity and reduced fracturing.

The method's accuracy in detecting low-velocity zones (e.g., between 30–45 m and 65–85 m on L-1) highlights its utility for identifying potential fault zones.

These results validate the refraction seismic approach as a cost-effective and reliable tool for engineering geological investigations.

Acknowledgments

This paper was supported by the Guangdong Basic and Applied Basic Research Foundation (Grant No. 2023A1515012836), and Colleges Youth Innovative Talents Project of Guangdong Province (Grant No. 2022KQNCX080), Guangdong Provincial Department of Finance Project (Grant No. 2024A0505050030)., Research Startup Project of Jiaying University (Grant No. 2023RC69) and the Research Project (Grant No. 2023KJY01). Scientific research project in school-level (2023KJM01)

References

1. Shearer, P. M. Introduction to Seismology. Cambridge University Press. 1999. DOI: 10.1017/9781316877111
2. Telford, W. M., et al. *Applied Geophysics*. Cambridge University Press. 1990. DOI: 10.1017/CBO9781139167932
3. Lanz, E., Maurer, H., & Green, A. G. (1998). *Refraction tomography over a buried waste disposal site*. *Geophysics,* 63(4), 1414-1433.. DOI: 10.1190/1.1444443
4. Lankston, R. W. High-resolution refraction seismic data acquisition and interpretation. *Geotechnical and Environmental Geophysics*, 1990, *55*(5), 626–632. URL: https://library.seg.org/doi/abs/10.1190/1.9781560802785.ch3
5. Al-Heety, A.J.; Hassouneh, M.; Abdullah, F.M. Application of MASW and ERT methods for geotechnical site characterization: A case study for roads construction and infrastructure assessment in Abu Dhabi, UAE. J. Appl. Geophys. 2021, 193, 104408. DOI: 10.1016/j.jappgeo.2021.104408
6. Mohammed, M.A.; Abudeif, A.M.; Abd El-aal, A.K. Engineering geotechnical evaluation of soil for foundation purposes using shallow seismic refraction and MASW in 15th Mayo, Egypt. J. Afr. Earth Sci. 2020, 162, 103721. DOI: 10.1016/j.jafrearsci.2019.103721
7. Adewoyin, O.O.; Joshua, E.O.; Akinyemi, M.L.; Omeje, M.; Adagunodo, T.A. Evaluation of geotechnical parameters of reclaimed land from near-surface seismic refraction method. Heliyon 2021, 7, e06765. DOI: 10.1016/j.heliyon.2021.e06765
8. Cultrera, G.; Cornou, C.; Di Giulio, G.; Bard, P.Y. Indicators for site characterization at seismic station: Recommendation from a dedicated survey. Bull. Earthq. Eng. 2021, 19, 4171–4195. DOI: 10.1007/s10518-021-01136-7
9. Di Giulio, G.; Cultrera, G.; Cornou, C.; Bard, P.Y.; Al Tfaily, B. Quality assessment for site characterization at seismic stations. Bull. Earthq. Eng. 2021, 19, 4643–4691. DOI: 10.1007/s10518-021-01137-6